communications earth & environment

A Nature Portfolio journal

Article

https://doi.org/10.1038/s43247-026-03975-1

Rapid increase of climate extremes reveals new areas of concern in Amazonia

Check for updates

Jos Barlow[1,34] ✉, Nathália S. Carvalho[1,34] ✉, Cássio Alencar Nunes[1,34] ✉, Ana Paula Dutra Aguiar[2], Ane Alencar[3], Liana O. Anderson[33], Luiz E.O.C Aragão[2], Fabricio Baccaro[4,25], Mike Barrett[5], Erika Berenguer[6], Kristian Bodolai[7], Paulo Monteiro Brando[8], Thiago B. A. Couto[9], Tomas Ferreira Domingues[10], Fernando Elias[32], Ted R. Feldpausch[12], Igor José Malfetoni Ferreira[2], Joice N. Ferreira[11], Bernardo M. Flores[13], David Galbraith[14], Toby Alan Gardner[15], Emanuel Gloor[14], Marina Hirota[16], Valerie Kapos[17], David M. Lapola[18], Cecília Leal[1], Alexander Charles Lees[19], Bel Lyon[5], Marcia N. Macedo[20], Yadvinder Malhi[6], Beatriz Schwantes Marimon[21], Ben Hur Marimon Junior[21], Patrick Meir[22], Lina M. Mercado[12,31], Oliver Metcalf[1], Leonardo de Sousa Miranda[1], Edward T. A. Mitchard[7], Douglas C. Morton[23], Jeanne L. Nel[24], Rafael Silva Oliveira[18], Oliver L. Phillips[14], Lucy Rowland[12], Juliana Schietti[25], Camila V. J. Silva[3], Celso H. L. Silva-Junior[3,30], Patrícia S. Silva[8], Juliana M. Silveira[1], Divino Vicente Silvério[26], Stephen Sitch[12], Paulo Amador Tavares[27], Cristina Telhado[17], Ima C. G. Vieira[28] & Helga Correa Wiederhecker[29]

Amazonia is highly sensitive to climate extremes, yet we lack an Amazon-wide assessment that examines the spatial-temporal changes in these extreme conditions. We address this within seasons and across the hydrological year, using a quantiles approach that integrates the frequency and magnitude of climate extremes and by linking changes in temperature with evapotranspiration. We show that high temperature extremes and temperature-linked measures of water deficit are both changing at a much faster rate than central trends. The 95th percentile of maximum temperatures in the driest period increased by 0.49 °C per decade (dec^{-1}) compared to 0.21°C dec^{-1} for the central trend of mean temperatures for the year. Crucially, over 700,000 square kilometres in central-north Amazonia have experienced increases in extreme dry season temperatures ≥ 0.75 °C dec^{-1} (≥ 3.22 °C over 43 years). Adaptation measures for these rapid changes in climate extremes must include preventing the deforestation and disturbances that amplify risks.

The frequency and intensity of climate extremes have increased in many regions of the world[1] and are predicted to increase further under future climate change scenarios[2]. These extremes are responsible for some of the greatest climate-linked impacts on nature and people, driving increases in human morbidity and mortality[3,4], losses of forest species[5] and ecosystem degradation[6]. Climate extremes are also responsible for deleterious changes in some of the world's most important ecosystems. In Amazonia, recent exceptionally hot or dry periods have led to extensive and unprecedented forest fires[7–9], large-scale tree mortality[10], and localised animal mortality[11], extreme warming of waters[12], and negative outcomes for human access to services[13] and health[14–16]. An increase in the incidence and severity of climate extremes could therefore help push Amazonia past critical thresholds, leading to much larger-scale deterioration of social and ecological conditions[17–19].

Given the importance of climate extremes in Amazonia, it is crucial to understand the temporal and spatial distribution of change. Although the central trends of temperature change in Amazonia are tracking global averages[20–22], these are often poor predictors of the trends of climate extremes[1]. This is particularly the case in South America, where the divergences between changes in mean and extreme temperatures are widespread, but variable[1]. Inferences from global, pantropical or regional studies on changes in climate extremes are currently insufficient. Many report only annual averages, which are known to mask ecologically important seasonal changes[23]. Others simplify the substantial spatial and temporal heterogeneity in dry season length and onset that exists across Amazonia[24] (Supplementary Fig. 1) by defining dry season timing according to the drier period in the southern Amazon[20,25,26] or across large sub-regions[21,22,27]. In

A full list of affiliations appears at the end of the paper. ✉e-mail: jos.barlow@lancaster.ac.uk; nathalia.bioufla@gmail.com; cassioalencarnunes@gmail.com

addition, most focus on changes in either temperature, precipitation or water deficit, and therefore fall short of the integrated approach required to understand drivers of key ecological responses such as vegetation productivity and mortality[28] and forest flammability[29].

Here, we provide a comprehensive assessment of the changing central (50th percentile) and extreme trends (5th and 95th percentiles) of multiple climate variables across the 7 million km^2 region of Amazonia (see Methods), based on 11 km spatial resolution (57,900 grid cells) from 1981 to 2023 (43 years). Our analysis of extreme trends is not intended to identify particular extreme events as others have done[8,10,30], but instead, focuses on the trends in the tails of conditional distributions (climate variables over time). This approach provides an integrated way to understand the changes in both the frequency and the intensity of extreme events across the whole time series.

To do this, we first divide the year into 73 pentads to explore changes across hydrological years, following approaches used to identify changes in dry season timing across extensive subregions[22,31]. However, we extend this so that each grid square has its own hydrological periodicity, with annual or seasonal periods starting with the wettest pentad or month instead of calendar years or fixed months (Supplementary Fig. 2). This allowed us to assess daily averages of minimum, mean and maximum temperature and Vapour Pressure Deficit (VPD) during the driest period as well as across the hydrological year. For rainfall, we evaluated the driest and wettest periods and the intensification of the water cycle through changes in rainfall amplitude. We also integrate changes in temperature with changes in rainfall or humidity, analysing variation in VPD and Maximum Cumulative Water Deficit (MCWD) that are well-established predictors of both plant physiology and fire activity[30,32]. MCWD was calculated in two ways: using a fixed 100 mm of evapotranspiration per month commonly used in the literature[30,33] ($MCWD_{100}$) and by allowing evapotranspiration to increase with temperature ($MCWD_{Temp}$) following modelled estimates of temperature and atmospheric CO_2 responses[34] that are broadly supported by recent observations[35]. Finally, we identified the metrics and regions showing the greatest rates of change and also assessed whether higher rates of change are associated with historically warmer or drier conditions.

We show that Amazonia's climate has changed rapidly, but not uniformly. Extremes are changing at a much higher rate than central trends, and Amazonia-wide shifts in temperature—rather than precipitation—are driving most of the changes in water deficit and VPD. Crucially, we identified a hitherto under-emphasised and spatially distinct region of high climate change in the central-north Amazon. We discuss these results considering their implications for climate adaptation, conservation and sustainability in Amazonia.

Results and discussion

Climate change across Amazonia

On average, the rate of change of extreme temperatures from 1981 to 2023 was faster than the central trend (Fig. 1, Supplementary Fig. 3). For central trends, annual mean temperatures increased by a mean rate of 0.21 °C per decade (dec^{-1}), (Interquartile Range IQR: 0.15 °C–0.27 °C dec^{-1}) and 0.90 °C between 1981 and 2023, which is in line with the global average and previous estimates for Amazonia[20] (Fig. 1a). However, the 95^{th} percentile of mean temperatures increased at a mean rate of at least 0.30 °C dec^{-1} (IQR:0.24 °C–0.36 °C dec^{-1}) and 1.29 °C over 43 years (Fig. 1a). As expected, the rate of increase was greater in the driest period than across the whole hydrological year[21], with maximum temperature at the 95th percentile increasing by 0.49 °C dec^{-1} (IQR: 0.35 °C–0.63 °C dec^{-1}) (Fig. 1a). This corresponds to an increase of 2.11 °C over 43 years, 2.34 times higher than the annual mean central trend (Fig. 1a).

Temperature-linked measures of maximum cumulative water deficit ($MCWD_{Temp}$) and the vapour pressure deficit (VPD) also showed large changes over time, with higher values for extreme percentiles. For VPD, increases in the 95th percentiles were about one-third higher than for the central trend, for both annual and driest periods (Fig. 1b). VPD also had the greatest rate of change during the driest period, increasing by 0.06 kPa dec^{-1} at the central trend (IQR: 0.02-0.09 kPa dec^{-1}) and 0.26 kPa over 43 years. This was even higher at the 95th percentile, increasing by 0.08 kPa dec^{-1} (IQR :0.04–0.12 kPa dec^{-1}; 0.34 kPa over 43 years) (Fig. 1b). For MCWD, which is scaled towards the negative, the 5th percentile represents the drier extreme. The mean rate of change at the 5th percentile of $MCWD_{Temp}$ was −12.75 mm dec^{-1} (IQR: −22.88 to −0.96 mm dec^{-1}) and −54.82 mm over 43 years. This was twice that of the central trend of $MCWD_{Temp}$ of −6.61 mm dec^{-1} and −28.42 mm over 43 years (Fig. 1c). The temperature-invariant measure of $MCWD_{100}$ showed no directional trend, with the 50th percentile changing by just 0.03 mm dec^{-1} (IQR: −5.13 to 4.01 mm dec^{-1}) and 0.13 mm over 43 years (Fig. 1c).

Precipitation increased across the central, 5th and 95th percentiles for both annual and wettest periods of the year, but the trends were close to zero when assessing only the driest period (Supplementary Fig. 3d). For the central trend, annual precipitation increased by a mean rate of 31.29 mm dec^{-1} (IQR: −8.14 to 65.28 mm dec^{-1}) and 134.55 mm over 43 years; Supplementary Fig. 3d). Precipitation amplitude showed a slight increase at all percentiles, with the greatest at the 95th percentile, where intensification of the water cycle—the difference between the wettest and driest periods—rose by a mean rate of 14.95 mm dec^{-1} (IQR: −19.29 to 51.42 mm dec^{-1}) or 64.28 mm over 43 years (Supplementary Fig. 3e).

Spatial variation and hotspots of climate change

Amazonia-wide averages encompass considerable regional variation, with pronounced spatial divergence among the regions most affected by the highest rates of change at the 50th and extreme percentiles (Fig. 2, Supplementary Figs. 4–8). For the central trend of change across the hydrological year, our results are broadly consistent with previous work, and the southern Amazon stands out as the region most affected by increases in temperature and temperature-linked variables such as VPD (Fig. 2 and Supplementary Figs. 4, 5)[21,36]. However, at the 95th percentile, the greatest rates of change for temperature and VPD are concentrated in a central-northern region (Fig. 2a, b) that has rarely been identified as being imperilled by climate change. Here, changes in average maximum temperature and mean VPD in the driest period were particularly alarming, with 10% of the biome surpassing rates of increase of 0.75 °C dec^{-1} (> 3.22 °C over 43 years) and 0.14 kPa dec^{-1} (> 0.60 kPa over 43 years). The region was also a locus of change in $MCWD_{temp}$, with extreme years seeing rates of change of −35.02 mm dec^{-1} (< −150.59 mm over 43 years) (Fig. 2).

There was a strong spatial signal to the difference between central and extreme rates of climate change (Fig. 3). In much of the southern and southeastern Amazon, central trends are growing at a similar rate to—or even slightly faster than—the 95th percentile of temperature and VPD or 5th percentile of $MCWD_{temp}$. In contrast, in the central-north region the rate of change of climate extremes (95th percentiles for temperature and VPD, 5th percentiles for $MCWD_{temp}$) diverged greatly from both the central trends and the opposite extremes (Fig. 3a). Overlaying the top deciles of rates of change at the central and most extreme trends (95th percentile for mean temperature in the hydrological year, maximum temperature and VPD in the driest period of the hydrological year with the 5th percentile for $MCWD_{Temp}$) highlights critical regions where the fastest rates of change are co-occuring (Fig. 4). For central trends, there was strong spatial agreement between temperature and VPD, while $MCWD_{Temp}$ was also prevalent on the southern borders of Amazonia. For the extreme trends, temperature-VPD overlaps were also extensive, but critical areas for $MCWD_{Temp}$ included additional regions at the periphery of Amazonia (Fig. 4). These regions of greatest risk from rising central and extreme trends are predominantly located within Brazil and overlap with many important protected areas and indigenous lands (Supplementary Fig. 9).

Linking climate change to historical averages

Given the strong spatial signal of the observed climate trends, we investigated whether central or extreme trends were spatially associated with the historical averages from the start of the time series (1981–1990; Supplementary Fig. 10). The data were variable across metrics, and most

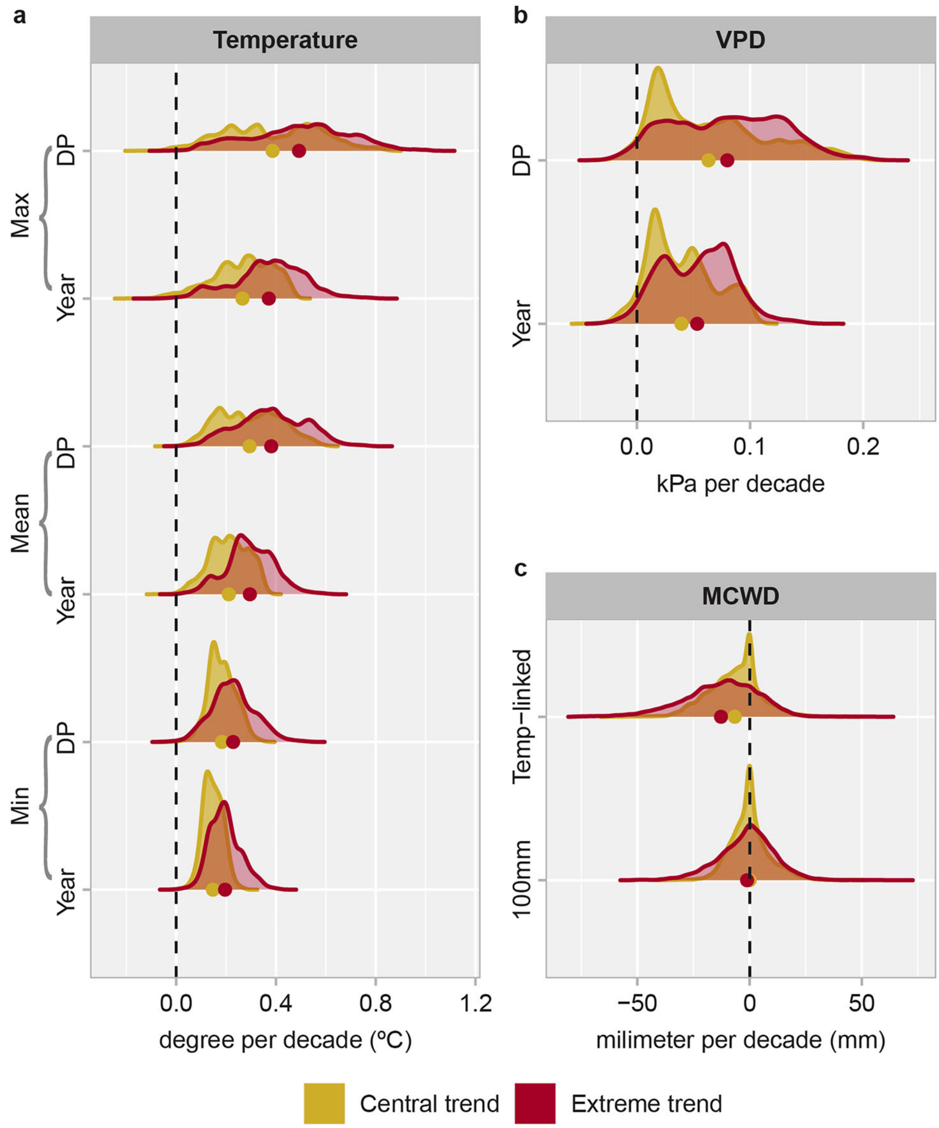

Fig. 1 | The magnitude of climate change across the Amazon region over 43 years (1981-2023). Decadal rates of change of (**a**) temperature (°C per decade) (**b**) vapour-pressure deficit (VPD; kPa per decade) and (**c**) maximum cumulative water deficit (MCWD; mm per decade). All panels show the rate of change for the central trend (50th percentile) and extreme (95th percentile for temperature and VPD; 5th percentile for MCWD), calculated on grid cell-wise with a spatial resolution of 11 km. Trends for minimum, mean and maximum temperature and mean VPD were calculated for the hydrological year (Year) and driest period (DP) considering pentad means (5-day period). MCWD was calculated considering two evapotranspiration (ET) thresholds, one fixed at 100 mm and the other linked to temperature. In all panels, coloured dots represent the Amazon-wide mean rate of change per decade for each variable in each period for the central (yellow) and extreme (red) trends. Black dashed vertical lines correspond to zero. The panel for all variables is available in Supplementary Fig. 3.

correlation coefficients were generally non-significant (Supplementary Fig. 10). However, central trends were more positively associated with historical averages than the extreme trends, and there was a significant positive internal association between rates of change at the 50th percentile and the historical climate for $MCWD_{Temp}$ ($r = 0.38$) and for VPD measured across the hydrological year ($r = 0.27$) and in the driest period ($r = 0.34$). These associations indicate that regions with historically higher MCWD and VPD are experiencing the highest rates of change for central trends.

Sensitivity of results to the 2023–24 extreme event

As our time series ends in an extreme year (2023–24), we assessed whether this event was driving the findings from the full time series (Supplementary Methods, Supplementary Fig. 11). For central trends, there was very strong agreement between the rates of changes calculated for both periods across all climate metrics ($r = 0.98$–0.996). These correlations were weaker for extreme percentiles ($r = 0.78$–0.91) and, as expected, removing the most recent extreme event lowers the magnitude of change (Supplementary Fig. 11). However, the main spatial trends were not sensitive to removing 2023–24 from the time series, and the central-northern region retained the highest rates of change in 95th percentiles of maximum dry-season temperatures and VPD as well as highest rates of change in the 5th percentile of $MCWD_{Temp}$ (Supplementary Fig. 11).

A new region of climate concern

While the southern Amazon is confirmed as the fastest-warming region on average, it is the central-northern region that is experiencing the greatest rates of increase in extreme temperature and VPD. This central-northern region is a critical part of Amazonia's cultural and biological wealth, encompassing extensive areas of high forest cover, native savannas, and key indigenous territories, including the Coata-Laranjal, Waimiri-Atroari, Yanomami and Trombetas/Mapuera (Supplementary Fig. 9). The historical record of maximum temperatures (Supplementary Fig. 4) and water deficit (Supplementary Fig. 6) suggests this region has experienced less extremely hot or dry conditions than forests in south and eastern Amazonia. Multiple lines of evidence demonstrate that climate extremes are already affecting socio-ecological systems in this central-northern region. Examples include the first observed mass mortality of forest mammals in Amazonia[11] and the loss of understorey bird populations and changes in bird lifespans, behaviour and morphology[37–39]. Aquatic systems have undergone extreme reductions in surface water[40] and abrupt shifts in fish assemblages[41]. Extreme heat and water deficit have contributed to extensive forest fires in the Brazilian state of Roraima[42] and in flooded forests along the Rio Negro[43]. These and other fire events have likely contributed to record levels of air pollution and hospitalisations in the largest Amazonian urban centre of Manaus[44,45].

The drivers of the increase in extremes in the central-northern region require further investigation. The record drought of 2023/24 provides

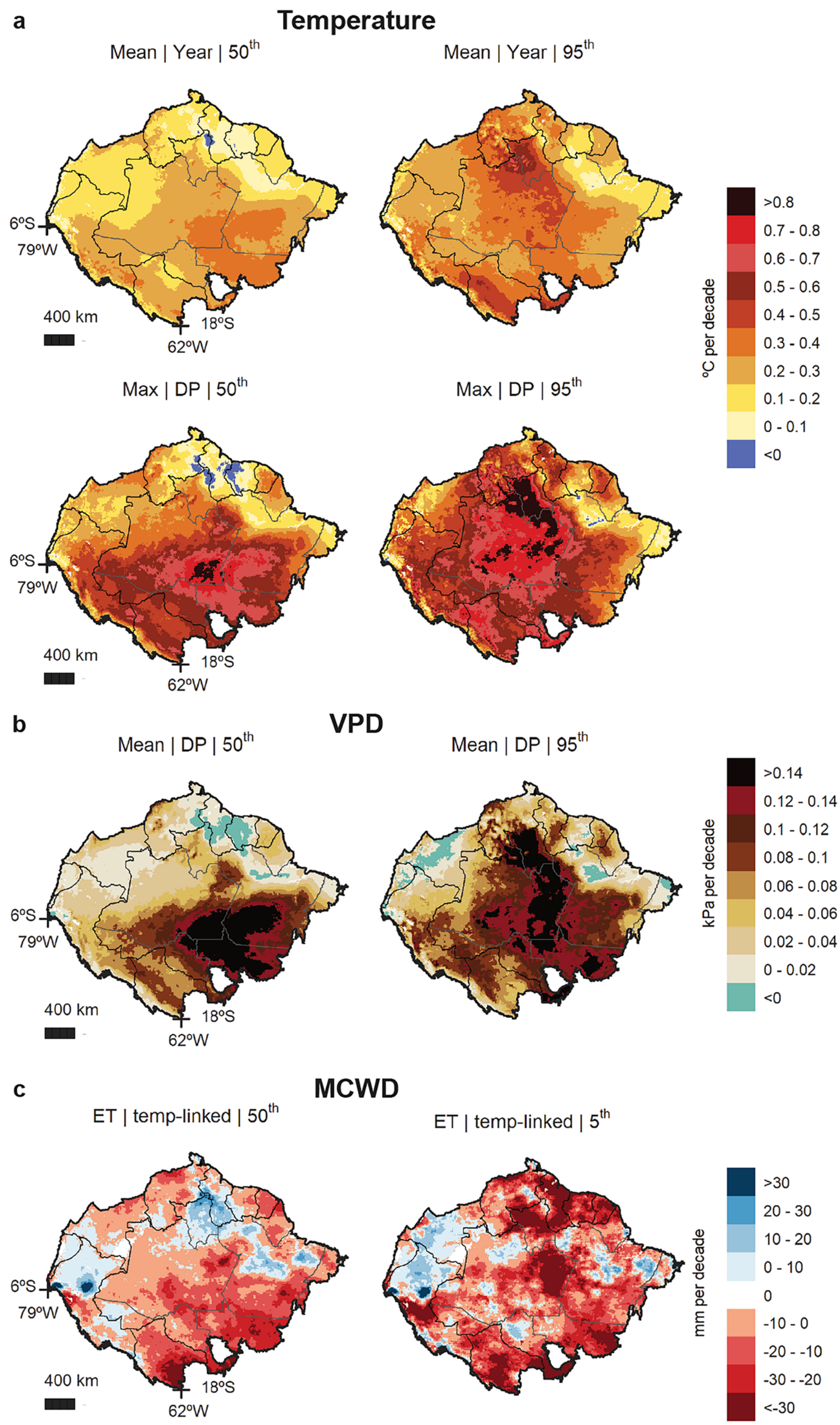

Fig. 2 | Spatial distribution of climate change across the Amazon over 43 years (1981–2023). Decadal rates of change were calculated grid cell-wise at 11 km spatial resolution for (**a**) the mean and maximum temperature (**b**) mean vapour-pressure deficit (VPD) and (**c**) maximum cumulative water deficit (MCWD). The rates of change for temperature (°C per decade) and VPD (kPa per decade) are shown, along with both the central (50th) and upper extreme (95th percentile) trends, for the hydrological year (Year) and the driest period (DP). For MCWD, the rate of change is shown for the central trend (50th percentile) and the lower extreme (5th percentile) considering a temperature-linked evapotranspiration threshold. Maps for all variables, percentiles and periods are available in Supplementary Figs. 4–8.

insights, as the low rainfall and high temperatures in the northern Amazon were linked to sea surface temperature (SST) anomalies in the eastern tropical and central equatorial Pacific relating to the transition from La Niña to El Niño conditions[26]. The region has also been identified as being at risk from major global climatic events, such as a slowing down of the Atlantic Meridional Overturning Circulation (AMOC)[46] or changes in cloud cover linked to a narrowing of the Intertropical Convergence Zone[47]. However, the extent of these changes remains uncertain[48,49]. Changes in soil moisture have been shown to exert a strong influence on extreme temperatures in regional hotspots of warming[50], but much of the central-northern region has experienced increases in annual and dry-period precipitation (Supplementary Fig. 7), and soils are variable and not consistently different from those in regions where extremes have changed less[51].

Regardless of the underlying cause, the high rate of increase of extreme temperatures, VPD and water deficits demonstrates the critical importance of preventing further frontier advance in this region. Additional deforestation would amplify temperature changes and expose the remaining forests to heightened fire risks exacerbated by edge creation, within-forest disturbances, such as logging, and the spread of ignition sources[17,52]. Sustained investment in adaptation will be required[53],

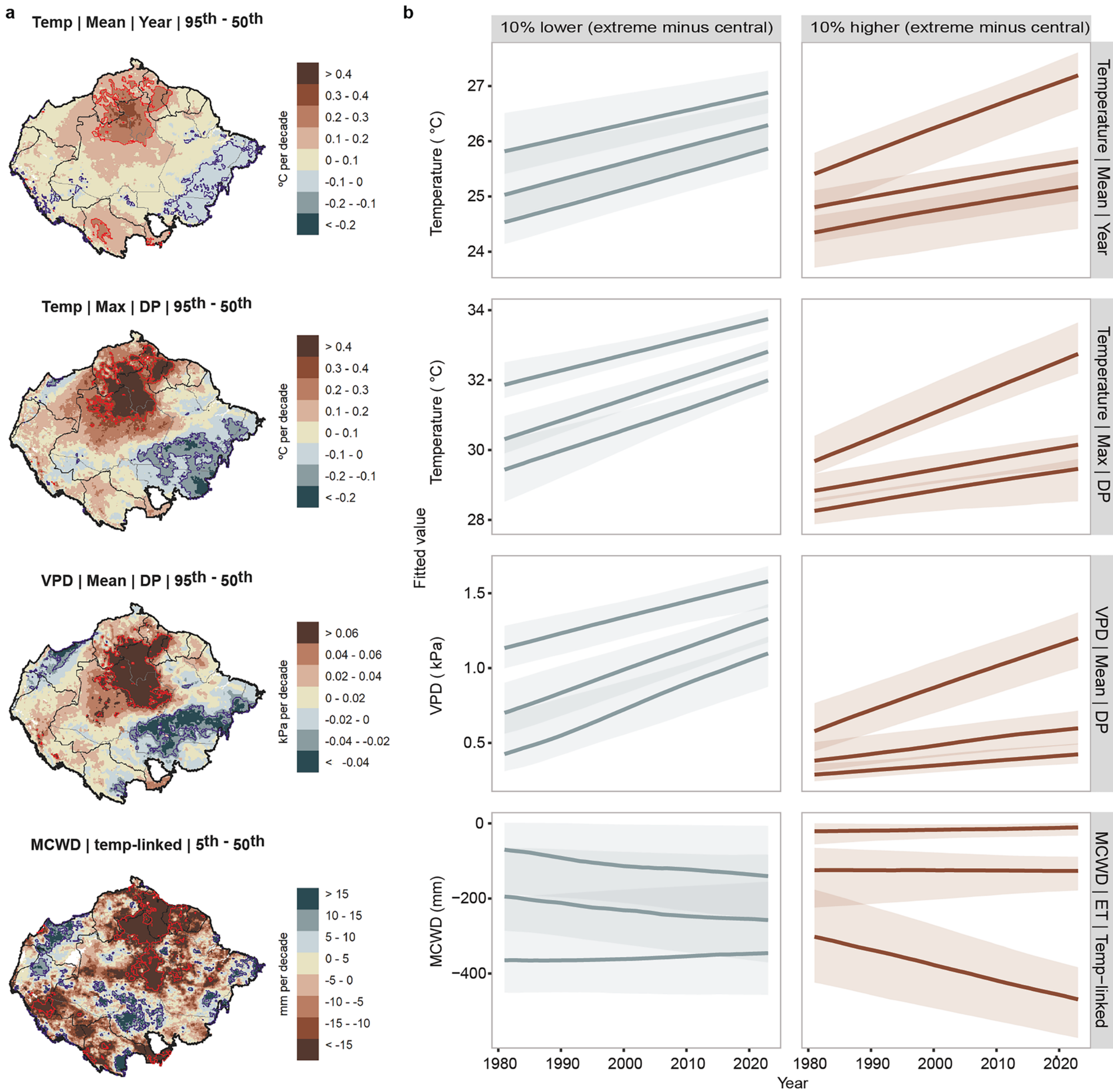

Fig. 3 | Spatial difference in the slope of change between extreme and central percentiles, highlighting trends of change in regions with the highest and lowest values differences. a Difference between the rate of change in extreme and central (50th percentile) trend was calculated per cell for mean temperature (hydrological year, 95th percentile), maximum temperature (driest period, 95th percentile), vapour-pressure deficit (VPD, driest period, 95th percentile) and maximum cumulative water deficit (MCWD, temperature-linked, 5th percentile). In all maps, the brown scale indicates faster rate of change in the extreme, while the blue scale indicates faster rate of change in the central trend. **b** trends of change in regions with the highest (outlined in red on maps) and lowest (outlined in purple on maps) values of differences between the slope of change of extreme and central percentiles. The region with the 10% highest values is where the extreme slopes of change are greater than the central slopes of change and vice-versa. Graphs show the trends of change in mean and maximum temperature, VPD and temperature-linked MCWD from 1981 to 2023 in both regions. Lines represent the median curves for 5th, 50th, and 95th percentiles and shaded areas around the lines represent the interquartile range (IQR) +/- 25% - i.e., the dispersion of 50% of all curves.

particularly where preexisting infrastructure and development deficiencies exacerbate people's vulnerability and the risks to health[54], well-being in urban environments[15,45], and the viability of sustainable socio-bioeconomies[55,56]. Support will also be required to maintain the viability of some of the key climate change and conservation interventions, as the increase in extreme climate conditions jeopardises both protected areas through megafires[57] and the regrowth of secondary forests[58,59]. All of this will require improvements in monitoring to evaluate risks and identify the most effective adaptation approaches.

Precipitation changes and uncertainty

There was no clear signal of strong reductions in precipitation across Amazonia or major differences between central and extreme trends. The only region where rainfall declined significantly in our analysis (Supplementary Fig. 7) and in other studies[18,60] was small and bisected the Brazilian states of Rondônia and Amazonas. In fact, overall, there was a slight increase in biome-wide averages. This could reflect increased moisture arriving from the warming tropical Atlantic Ocean[23,61,62] acting to offset the local and regional losses of precipitation resulting from deforestation[27,63].

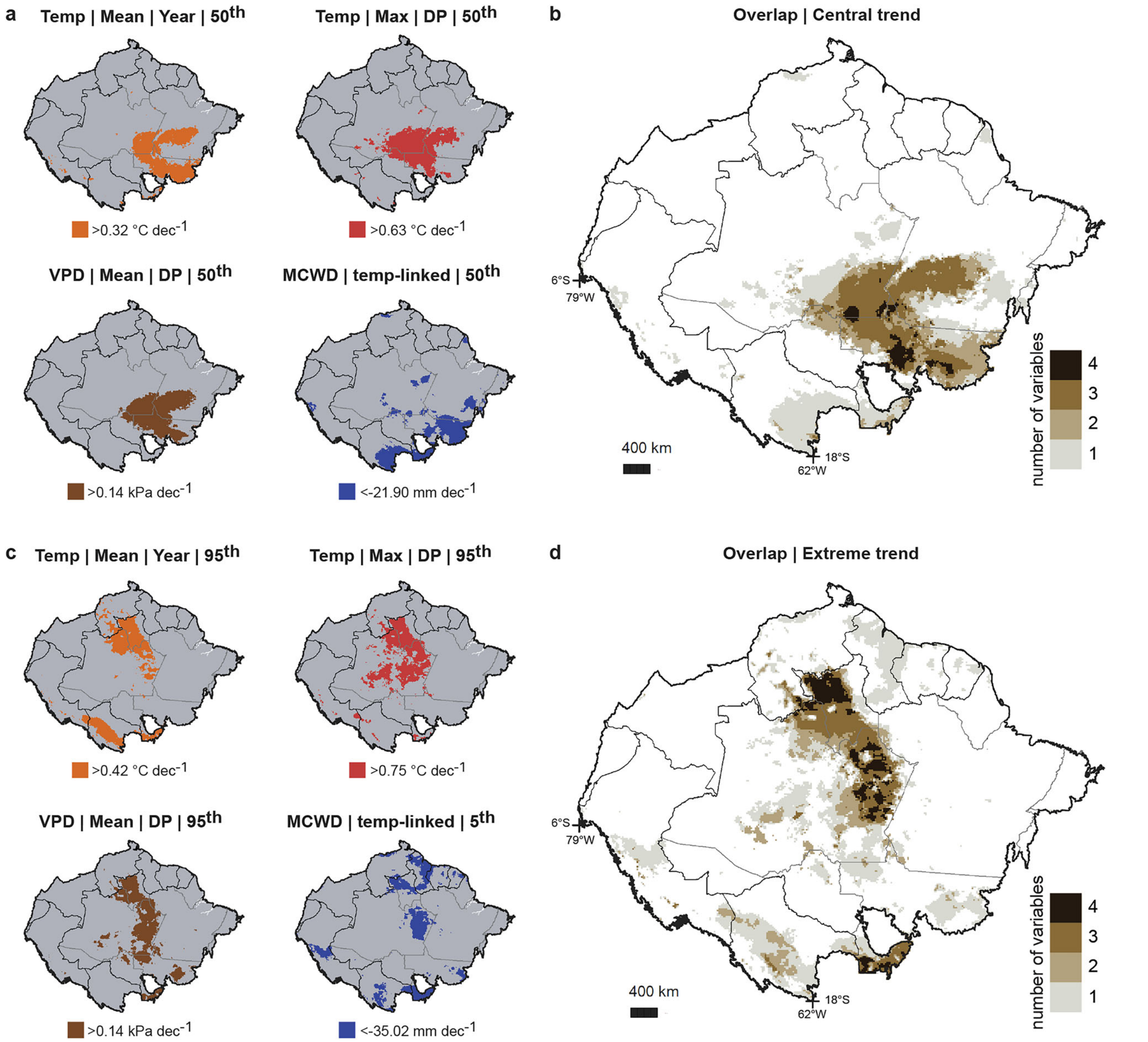

Fig. 4 | Critical areas with the highest rate of change in the central trend and extremes. Regions within the 10% top values of decadal rate of change in the (**a**) central trend and (**b**) extreme (95th percentile for mean temperature in the hydrological year, maximum temperature and mean vapour-pressure deficit (VPD) both in the driest period (DP); 5th percentile for maximum cumulative water deficit (MCWD) with temperature-linked. (**c**) Overlap of all variables for central trend and (**d**) extremes, ranging from one to four overlapping variables.

The lack of a wider decline of rainfall in southern Amazonia contrasts with research based on rainfall gauges and other rainfall reanalysis products that identify a strong and consistent drying signal across a similar period[31,36]. Although satellite products can underestimate periods of high rainfall and dry days[64], CHIRPS is considered one of is the best products for tropical precipitation during extreme climate events[65] and is even more accurate in drier regions of the Amazon[64], where the greatest drying trend has been identified in other studies[36]. Furthermore, the overall increase in rainfall detected by CHIRPS is consistent with increased river flows[23] and groundwater storage[66]. In contrast, the signal from rainfall gauges used in previous work[31] is difficult to interpret due to their sparse coverage[67], inconsistent directional trends across stations[68,69], and their biased distribution towards the most deforested areas[70] and along rivers where the breeze influences rainfall[71]. As such, the source of the relatively low correlation between CHIRPS and Gauges (54%, see Supplementary Fig. 12) is unclear, as gauges are also beset by uncertainties, highlighting the importance of improving the observational network across tropical South America[69].

Temperature drives changes in indices of water stress

Overall, changes in temperature rather than precipitation are driving the most significant increases in VPD and reductions in $MCWD_{Temp}$, with the greatest recorded changes in the central-north region occurring where there is a good coverage of weather stations[69] to inform and constrain climate reanalysis data (Supplementary Figs. 13–15). However, the large difference between our temperature-invariant and temperature-linked measures of water deficit highlights the urgent need to reduce uncertainty around temperature and CO_2 effects on evapotranspiration in tropical forests. Elevated CO_2 induces stomatal closure, causing plants to reduce transpiration under elevated CO_2[72,73]. Malhi et al.[34] predict this reduction would be smaller than the temperature-induced increases in evaporation from the soil or transpiration from the leaf. Although other models suggest a stronger influence of CO_2 than temperature[74], an overall increase in evapotranspiration is consistent with the relationship between temperature and potential evapotranspiration in the Penman-Monteith model[75] and from models and remote sensing observations conducted across the arc of deforestation[35]. Furthermore, our use of 8.9 mm for every degree increase in temperature[34] is potentially conservative compared to the observed 11% increase in dry season ET over the arc of deforestation over 23 years, when mean temperatures increased by c. 0.40 °C (Supplementary Fig. 4) and a higher increase in ET was offset by forest loss[35].

While our results demonstrate the importance of incorporating ET in the assessment of MCWD, many uncertainties remain in moving beyond the fixed ET threshold of 100 mm month^{-1} that has been the established estimate of evapotranspiration in tropical forests for the past two decades[10,30]. Changes in evapotranspiration are likely to be spatially variable[66], will vary across years and seasons[34], and may be sensitive to forest disturbances[76] as well as the drought indicator and data sources that are used[77]. While ET estimates based on remote sensing can reduce uncertainty, the marked divergence between products[78] will only be resolved with further validation and ground-based measures. In addition, remote sensing estimates actual ET – which often summarises multiple land use land cover classes – while MCWD is based on potential ET.

Conclusion

We show that climate change in Amazonia is neither gradual nor homogeneous, and that public policies must address the enormous challenge of rapidly increasing extreme temperatures and water deficits. Crucially, these are occurring in the central-northern region, far from the arc of deforestation. This spatial dissociation with the main loci of forest loss—the main local driver of climate change[27]—demonstrates that the world's highest greenhouse gas-emitting countries bear a strong responsibility for Amazonia's rapidly changing socio-ecological condition. This underscores once again the urgent need for rapid reductions in greenhouse gas emissions[2], which are projected to amplify the region's hydrological instability[79], and strengthens arguments that high-emitting countries should contribute to adaptation and conservation interventions in tropical forest regions through mechanisms such as the Fund for responding to Loss and Damage or novel initiatives such as the Tropical Forest Forever Facility. It is vital that this support reaches the most vulnerable regions and peoples and prevents further frontier advance that could amplify the consequences of climate extremes.

Methods

Datasets of climate variables

We used the following climate variables and resampling procedures to undertake our assessment of climate change in the Amazon region delimited by ref. 80.

Temperature and vapour pressure deficit (VPD). We used the ERA5-Land post-processed daily statistics dataset with 1-hour sub-daily frequency sampling over a 44-year period (1981-2024). We use 1981 as the starting point to standardise with precipitation data availability, and because 1981 is after the widely observed change in the rate of climate change that occurred in the 1970s[65,81]. ERA5-Land is a global climate reanalysis product produced by the European Centre for Medium-Range Weather Forecasts (ECMWF) available at a spatial resolution of 0.1° – approximately 11 × 11 km[82]. For temperature metrics, we used the 2-m temperature minimum, mean and maximum daily statistics. We calculated the mean VPD using the '*plantecophys*' R package[83,84], combining the ERA5-Land daily mean statistics from 2 m temperature, 2 m dewpoint and surface pressure.

Precipitation. We used the daily Rainfall Estimates from Rain Gauge and Satellite Observations (CHIRPS v2) dataset over a 44-year period (1981 to 2024). The CHIRPS algorithm integrates satellite data, ground-based observations and precipitation estimates to produce rainfall time series at a spatial resolution of 0.05°[85]. CHIRPS has been described as one of the most accurate datasets to represent the rainfall regime across Amazonia, demonstrating superior performance compared to other data sources when validated against station-based observations[86,87]. Validations across the basin have shown accuracy above 70%[68,88,89]. We resampled the CHIRPS dataset using bilinear interpolation to match the 0.1° spatial resolution of the ERA5-Land dataset.

Maximum cumulative water deficit (MCWD). We used CHIRPS to calculate the annual maximum cumulative water deficit (MCWD) from 1981 to 2024, an indicator of water stress in forests (Aragão et al., 2007). A water deficit occurs when evapotranspiration (ET) exceeds precipitation, with a 100 mm per month (month^{-1}) ET threshold commonly applied for tropical forests[30]. However, increases in temperature have affected Amazonia's ET by increasing atmospheric evaporative demand[34]. To incorporate this warming effect, we calculated MCWD using fixed 100 mm month^{-1} ET ($MCWD_{100}$) and temperature-linked ET ($MCWD_{temp}$). In this case, we considered that for each 1 °C above the mean temperature of a reference period (1971–1980), the 100 mm month^{-1} ET threshold is increased by 8.9 mm month^{-1}. This coefficient is based on simple linear extrapolations of simulations of climatic scenarios that predict an increase of evapotranspiration in the Amazon forest to 140 mm month^{-1} under conditions of increased temperature (4.7 °C) and CO_2 (850 ppm)[34]. Rescaling this adds 8.9 mm month^{-1} for every 1 °C increase in temperature, assuming atmospheric CO_2 concentrations and temperature increase linearly as per the model. We calculated the MCWD for both the fixed-ET ($MCWD_{100}$) and temperature-linked ET ($MCWD_{temp}$) using the R routine developed by ref. 90.

Determining the hydrological year

To assess trends in the climate variables, we defined a cell-wise hydrological year that follows Amazonia's highly variable precipitation cycle[24] rather than a fixed (January-December) calendar year or predetermined months. This approach considers the pronounced spatiotemporal variation in the timing and length of wet/dry periods across Amazonia. First, we aggregated the daily CHIRPS precipitation into 5-day periods (pentads), resulting in 73 pentads for each calendar year from 1981 to 2024. Leap days were removed from the analyses. Then, for each cell, we calculated the annual mean precipitation of each pentad over the 44-year period and identified the pentad with the highest mean precipitation. For each cell, the pentads of the calendar year were reordered according to the position of the wettest peak pentad, becoming the first of the 73 pentads of each hydrological year. For example, if the wettest pentad occurs in position 32 in the calendar year, the hydrological years for that cell span from pentad 32 of the current year (t) to pentad 31 of the next year ($t + 1$), (Supplementary Fig. 2).

We aggregated the daily statistics for the minimum, maximum, and mean temperature and mean VPD into mean 5-day periods (pentads) and reordered these variables according to the hydrological year. For MCWD, we applied the same methodology, but as this metric is calculated based on monthly thresholds for evapotranspiration, the hydrological years were defined based on the month with the highest precipitation. Because the wettest pentad/month generally did not occur in the first pentad/month of the calendar year, the hydrological year covered periods that extended across two calendar years in 99.84% of cells in the pentad approach and in 84.31% in the monthly approach, demonstrating the unsuitability of calendar years for these assessments. As a result, even though the CHIRPS and ERA5-Land datasets were available for 44 years (1981–2024), only 43 complete hydrological years were available for trend analysis (1981–2023).

Determining the driest and wettest periods of the year

To consider the spatiotemporal variation of precipitation across Amazonia[24], we used the CHIRPS hydrological year time series to identify the driest period for each cell. To identify the onset and end of the driest period, we applied the methodology proposed by ref. 31, comparing the mean precipitation of each pentad with the annual mean precipitation over the 43-year period. The onset corresponds to the first pentad in a sequence of at least six out of eight consecutive pentads with precipitation below the baseline. Conversely, the end of the driest period corresponds to the first pentad in a sequence of at least six out of eight with precipitation above the baseline (Supplementary Fig. 1). The wettest period was defined as all pentads outside the driest period.

Data analysis

Set of variables analysed

We calculated mean values for the entire hydrological year and for the driest period for temperature variables (minimum, mean and maximum) and for mean VPD. For MCWD, we calculated the values for the entire hydrological year. For precipitation, we obtained the annual sum and the sum for both driest and wettest periods. The precipitation in the wettest period was calculated as the difference between the precipitation in the hydrological year and the driest period. Finally, we calculated the precipitation amplitude by taking the difference between precipitation in the wettest and driest periods within the hydrological year.

Central and extreme trend analyses

To analyse central and extreme trends in climatic variables over time, we used non-parametric Quantile Generalised Additive Models (qGAM). We chose this model because it allowed us to test and obtain coefficients for central and extreme trends through percentile (*i.e.*, quantile) models, while still accounting for the temporal dependence of the data (analysis over years). To keep the trend analysis linear, we did not include a smoothing parameter for the term "hydrological year" [Response ~ hydrological year (1981-2023)]. For each cell and each variable, we ran a qGAM for the 50th (median – central) and 5th and 95th (extremes) percentiles and obtained the coefficients, which can be interpreted as the rates of change of a given variable (change in the variable per year). We did that using the function '*qgam*' from R package '*qgam*'[91] version 2.0.0 in the R software[84] version 4.5.1.

To pinpoint the areas with greatest divergence between extreme and central trends, we subtracted the values of the decadal rates of change in the 50th percentile from the rates of change in the extreme (95^{th} percentile for temperature and VPD and 5th percentile for $MCWD_{temp}$) for mean temperature in the hydrological year, maximum temperature and VPD in the driest period of the hydrological year and $MCWD_{Temp}$ of the hydrological year. We selected the top and bottom 10% values of the difference between central and extreme rates of change (i.e., 10% values for where extreme trends were higher than central trends and vice versa) to display the average curves for the regions with greatest divergence between extreme and central trends. For this, we built the trend curves (50th and 5th / 95th percentiles) for all the 5790 cells (10% of cells – 5,735 cells for MCWD) based on their intercepts and coefficients and calculated the median curve and IQR (25-75 – 50% of the data distribution). To identify overlaps between regions with the highest rates of change of different climate variables, we selected the top 10% values of decadal rates of change for mean and maximum temperature, VPD and $MCWD_{temp}$ of the extreme (95th percentile for temperature and VPD and 5th percentile for $MCWD_{temp}$) and central (50th percentile) trends.

Associations of rates of change with climatic initial conditions

To investigate if climate change is spatially associated with the average climatic conditions at the start of the time series, we ran 1000 bootstrap analyses of Spearman correlation, using 100 samples (cells) each time. We used the bootstrap approach because i) we wanted to have a confidence interval for the coefficients of correlation, ii) there is high spatial autocorrelation in the data, and iii) using > 50,000 points would increase the chances of type I error. We first calculated the mean values for each climatic variable in the period between 1981 and 1990. Then, for each combination of a variable, a percentile (5th, 50th and 95th), a period (year, Driest Period - DP and Wettest Period - WP) and a method (100 mm threshold and Temp-linked threshold for MCWD) we used the '*cor.test*' function in R software to bootstrap the Spearman correlation test and obtained the coefficient of correlation (r) between the rate of change and the mean value (1981–1990) of a given variable. We defined the confidence intervals as the distribution of 95% of the r coefficients (2.5th–97.5th percentiles) obtained from the 1000 bootstraps. We defined non-significant correlations as those whose confidence intervals crossed zero.

Data availability

All the data generated in this study is available in Zenodo repository: https://doi.org/10.5281/zenodo.21841170. ERA5-Land post-processed daily statistics dataset is available at: https://cds.climate.copernicus.eu/datasets. CHIRPS rainfall data is available at: https://www.chc.ucsb.edu/data/chirps. Maps of rates of change presented in this manuscript can be visualised interactively at: https://nathaliacarvalho.shinyapps.io/climate-extremes-amazonia/.

Code availability

The R scripts developed to run analysis and create the figures of this study are available in Zenodo repository: https://doi.org/10.5281/zenodo.21841170.

Received: 13 May 2026; Accepted: 18 August 2026;
Published online: 10 September 2026

References

1. Huntingford, C. et al. Acceleration of daily land temperature extremes and correlations with surface energy fluxes. *npj Clim. Atmos. Sci.* **7**, 84 (2024).
2. Dosio, A., Mentaschi, L., Fischer, E. M. & Wyser, K. Extreme heat waves under 1.5 °C and 2 °C global warming. *Environ. Res. Lett.* **13**, 054006 (2018).
3. Ebi, K. L. et al. Extreme Weather and Climate Change: Population Health and Health System Implications. *Annu. Rev. Public Health* **42**, 293–315 (2021).
4. IPCC, I. P. on C. C. G. et al. Health, Wellbeing and the Changing Structure of Communities. in *Climate Change 2022 – Impacts, Adaptation and Vulnerability* (eds. Pörtner, H.-O. et al.) 1041–1170 https://doi.org/10.1017/9781009325844.009.(Cambridge University Press, 2023).
5. Kotz, M., Amano, T. & Watson, J. E. M. Large reductions in tropical bird abundance attributable to heat extreme intensification. *Nat. Ecol. Evol*. https://doi.org/10.1038/s41559-025-02811-7.(2025).
6. Maxwell, S. L. et al. Conservation implications of ecological responses to extreme weather and climate events. *Divers. Distrib.* **25**, 613–625 (2019).
7. Alencar, A., Brando, P. M., Asner, G. P. & Putz, F. E. Landscape fragmentation. *Sev. Drought N. Amazon. For. Fire Regime Ecol. Soc. Am.* **25**, 1493–1505 (2015).
8. Aragão, L. E. O. C. et al. 21st Century drought-related fires counteract the decline of Amazon deforestation carbon emissions. *Nat. Commun.* **9**, 536 (2018).
9. Berenguer, E. et al. Tracking the impacts of El Niño drought and fire in human-modified Amazonian forests. *Proc. Natl. Acad. Sci.* **118**, e2019377118 (2021).
10. Bennett, A. C. et al. Sensitivity of South American tropical forests to an extreme climate anomaly. *Nat. Clim. Chang.* **13**, 967–974 (2023).
11. Guimaraes, A. F. et al. Extreme drought and heat lead to alarming mortality of Amazon fauna. *Acta Amazon*. **55**, 1590 (2025).
12. Fleischmann, A. S. et al. Extreme warming of Amazon waters in a changing climate. *Science* **390**, 4029 (2025).
13. Santos de Lima, L. et al. Severe droughts reduce river navigability and isolate communities in the Brazilian Amazon. *Commun. Earth Environ.* **5**, 370 (2024).
14. Machado-Silva, F. et al. Drought and fires influence the respiratory diseases hospitalizations in the Amazon. *Ecol. Indic.* **109**, 105817 (2020).
15. Campanharo, W. A., Morello, T., Christofoletti, M. A. M. & Anderson, L. O. Hospitalization Due to Fire-Induced Pollution in the Brazilian Legal Amazon from 2005 to 2018. *Remote Sens.* **14**, 69 (2021).

16. Libonati, R. et al. Drought–heatwave nexus in Brazil and related impacts on health and fires: a comprehensive review. *Ann. N. Y. Acad. Sci.* **1517**, 44–62 (2022).
17. Lapola, D. M. et al. The drivers and impacts of Amazon forest degradation. *Science* **379**, 8622 (2023).
18. Flores, B. M. et al. Critical transitions in the Amazon forest system. *Nature* **626**, 555–564 (2024).
19. Brando, P. M. et al. Tipping points of Amazonian forests: beyond myths and toward solutions. *Annu. Rev. Environ. Resour.* **247**, 17 (2025).
20. Jiménez-Muñoz, J. C., Sobrino, J. A., Mattar, C. & Malhi, Y. Spatial and temporal patterns of the recent warming of the Amazon forest. *J. Geophys. Res. Atmos.* **118**, 5204–5215 (2013).
21. Gatti, L. V. et al. Amazonia as a carbon source linked to deforestation and climate change. *Nature* **595**, 388–393 (2021).
22. Marengo, J. A. et al. Long-term variability, extremes and changes in temperature and hydrometeorology in the Amazon region: a review. *Acta Amazon*. **54**, 980 (2024).
23. Gloor, M. et al. Intensification of the Amazon hydrological cycle over the last two decades. *Geophys. Res. Lett.* **40**, 1729–1733 (2013).
24. Carvalho, N. S. et al. Spatio-temporal variation in dry season determines the Amazonian fire calendar. *Environ. Res. Lett.* **16**, 125009 (2021).
25. Qin, Y., Wang, D., Ziegler, A. D., Fu, B. & Zeng, Z. Impact of Amazonian deforestation on precipitation reverses between seasons. *Nature* **639**, 102–108 (2025).
26. Espinoza, J.-C. et al. The new record of drought and warmth in the Amazon in 2023 related to regional and global climatic features. *Sci. Rep.* **14**, 8107 (2024).
27. Franco, M. A. et al. How climate change and deforestation interact in the transformation of the Amazon rainforest. *Nat. Commun.* **16**, 7944 (2025).
28. Tavares, J. V. et al. Basin-wide variation in tree hydraulic safety margins predicts the carbon balance of Amazon forests. *Nature* **617**, 111–117 (2023).
29. Ray, D., Nepstad, D. & Moutinho, P. Micrometeorological and canopy controls of fire susceptibility in a forested Amazon landscape. *Ecol. Appl.* **15**, 1664–1678 (2005).
30. Aragão, L. E. O. C. et al. Spatial patterns and fire response of recent Amazonian droughts. *Geophys. Res. Lett*. **34**, 028946 (2007).
31. Fu, R. et al. Increased dry-season length over southern Amazonia in recent decades and its implication for future climate projection. *Proc. Natl. Acad. Sci. USA* **110**, 18110–18115 (2013).
32. Brando, P. M. et al. Abrupt increases in Amazonian tree mortality due to drought–fire interactions. *Proc. Natl. Acad. Sci. USA* **111**, 6347–6352 (2014).
33. Silva Junior, C. H. L. et al. Fire responses to the 2010 and 2015/2016 Amazonian droughts. *Front. Earth Sci.* **7**, 1–16 (2019).
34. Malhi, Y. et al. Exploring the likelihood and mechanism of a climate-change-induced dieback of the Amazon rainforest. *Proc. Natl. Acad. Sci. USA* **106**, 20610–20615 (2009).
35. Laipelt, L. et al. Increased Amazon evapotranspiration since 1990 in a warming climate. *Environ. Res. Lett.* **20**, 104025 (2025).
36. Marengo, J. A., Jimenez, J. C., Espinoza, J.-C., Cunha, A. P. & Aragão, L. E. O. Increased climate pressure on the agricultural frontier in the Eastern Amazonia–Cerrado transition zone. *Sci. Rep.* **12**, 457 (2022).
37. Jirinec, V. et al. Morphological consequences of climate change for resident birds in intact Amazonian rainforest. *Sci. Adv.* **7**, 1743 (2021).
38. Avilla, S. S., Sieving, K. E., Anciães, M. & Cornelius, C. Phenotypic variation in a neotropical understory bird driven by environmental change in an urbanizing Amazonian landscape. *Oecologia* **196**, 763–779 (2021).
39. Wolfe, J. D. et al. Climate change aggravates bird mortality in pristine tropical forests. *Sci. Adv.* **11**, 8086 (2025).
40. Souza, C. M. et al. Amazon severe drought in 2023 triggered surface water loss. *Environ. Res. Clim.* **3**, 041002 (2024).
41. Röpke, C. P. et al. Simultaneous abrupt shifts in hydrology and fish assemblage structure in a floodplain lake in the central Amazon. *Sci. Rep.* **7**, 40170 (2017).
42. Xaud, H. A. M., Martins, F., da, S. R. V. & Santos, J. R. dos. Tropical forest degradation by mega-fires in the northern Brazilian Amazon. *Ecol. Manag.* **294**, 97–106 (2013).
43. Carvalho, T. C. et al. Fires in Amazonian blackwater floodplain forests: causes, human dimension, and implications for conservation. *Front. Forests Glob. Change* **4**, 755441 (2021).
44. Smith, L. T., Aragão, L. E. O. C., Sabel, C. E. & Nakaya, T. Drought impacts on children's respiratory health in the Brazilian Amazon. *Nat. Sci. Rep.* **4**, 1–8 (2014).
45. de Souza Tadano, Y. et al. Predicting health impacts of wildfire smoke in Amazonas basin, Brazil. *Chemosphere* **367**, 143688 (2024).
46. Akabane, T. K. et al. Weaker Atlantic overturning circulation increases the vulnerability of northern Amazon forests. *Nat. Geosci.* **17**, 1284–1290 (2024).
47. Tselioudis, G., Remillard, J., Jakob, C. & Rossow, W. B. Contraction of the world's storm-cloud zones the primary contributor to the 21st century increase in the Earth's sunlight absorption. *Geophys. Res. Lett*. **52**, 114882 (2025).
48. Terhaar, J., Vogt, L. & Foukal, N. P. Atlantic overturning inferred from air-sea heat fluxes indicates no decline since the 1960s. *Nat. Commun.* **16**, 222 (2025).
49. Voosen, P. Earth's clouds are shrinking, boosting global warming. *Science* **387**, 17–17 (2025).
50. Berg, A. et al. Impact of soil moisture–atmosphere interactions on surface temperature distribution. *J. Clim.* **27**, 7976–7993 (2014).
51. Quesada, C. A. et al. Soils of Amazonia with particular reference to the RAINFOR sites. *Biogeosciences* **8**, 1415–1440 (2011).
52. Barlow, J., Berenguer, E., Carmenta, R. & França, F. Clarifying Amazonia's burning crisis. *Glob. Chang. Biol.* **26**, 319–321 (2020).
53. Lapola, D. M. et al. Limiting the high impacts of Amazon forest dieback with no-regrets science and policy action. *Proc. Natl. Acad. Sci. USA* **115**, 11671–11679 (2018).
54. Andrade, L. et al. Health-related vulnerability to climate extremes in homoclimatic zones of Amazonia and Northeast region of Brazil. *PLoS One* **16**, e0259780 (2021).
55. Evangelista-Vale, J. C. et al. Climate change may affect the future of extractivism in the Brazilian Amazon. *Biol. Conserv.* **257**, 109093 (2021).
56. Tregidgo, D., Campbell, A. J., Rivero, S., Freitas, M. A. B. & Almeida, O. Vulnerability of the Açaí Palm to climate change. *Hum. Ecol.* **48**, 505–514 (2020).
57. Nóbrega Spínola, J., Soares da Silva, M. J., Assis da Silva, J. R., Barlow, J. & Ferreira, J. A. shared perspective on managing Amazonian sustainable-use reserves in an era of megafires. *J. Appl. Ecol.* **57**, 2132–2138 (2020).
58. Elias, F. et al. Assessing the growth and climate sensitivity of secondary forests in highly deforested Amazonian landscapes. *Ecology* **101**, 2954 (2020).
59. Heinrich, V. H. A. et al. Large carbon sink potential of secondary forests in the Brazilian Amazon to mitigate climate change. *Nat. Commun.* **12**, 1785 (2021).
60. Funatsu, B. M. et al. Assessing precipitation extremes (1981–2018) and deep convective activity (2002–2018) in the Amazon region with CHIRPS and AMSU data. *Clim. Dyn.* **57**, 827–849 (2021).
61. Espinoza, V., Waliser, D. E., Guan, B., Lavers, D. A. & Ralph, F. M. Global analysis of climate change projection effects on atmospheric rivers. *Geophys. Res. Lett.* **45**, 4299–4308 (2018).
62. Beveridge, C. F. et al. The Andes–Amazon–Atlantic pathway: a foundational hydroclimate system for social–ecological system sustainability. *Proc. Natl. Acad. Sci. USA*. **121**, e2306229121 (2024).
63. Smith, C., Baker, J. C. A. & Spracklen, D. V. Tropical deforestation causes large reductions in observed precipitation. *Nature* **615**, 270–275 (2023).

64. de Moraes Cordeiro, A. L. & Blanco, C. J. C. Assessment of satellite products for filling rainfall data gaps in the Amazon region. *Nat. Resour. Model*. **34**, 12298 (2021).
65. Burton, C., Rifai, S. & Malhi, Y. Inter-comparison and assessment of gridded climate products over tropical forests during the 2015/2016 El Niño. *Philos. Trans. R. Soc. B Biol. Sci.* **373**, 20170406 (2018).
66. Heerspink, B. P., Kendall, A. D., Coe, M. T. & Hyndman, D. W. Trends in streamflow, evapotranspiration, and groundwater storage across the Amazon Basin linked to changing precipitation and land cover. *J. Hydrol. Reg. Stud.* **32**, 100755 (2020).
67. Zhao, H. & Ma, Y. Evaluating the drought-monitoring utility of four satellite-based quantitative precipitation estimation products at global scale. *Remote Sens. (Basel)* **11**, 2010 (2019).
68. Paca, V. H., da, M., Espinoza-Dávalos, G., Moreira, D. & Comair, G. Variability of trends in precipitation across the Amazon River basin determined from the CHIRPS precipitation product and from station records. *Water* **12**, 1244 (2020).
69. Cattelan, L. G., Mattos, C. R. C. & Hirota, M. Unraveling divergences: disagreement between precipitation datasets and stations in tropical South America. *Environ. Res. Lett.* **20**, 104043 (2025).
70. Mu, Y. & Jones, C. An observational analysis of precipitation and deforestation age in the Brazilian Legal Amazon. *Atmos. Res.* **271**, 106122 (2022).
71. Fitzjarrald, D. R. et al. Spatial and temporal rainfall variability near the Amazon-Tapajós confluence. *J. Geophys. Res. Biogeosci*. **113**, 596 (2008).
72. De Kauwe, M. G. et al. Forest water use and water use efficiency at elevated CO2: a model-data intercomparison at two contrasting temperate forest FACE sites. *Glob. Chang. Biol.* **19**, 1759–1779 (2013).
73. Cernusak, L. A. et al. Environmental and physiological determinants of carbon isotope discrimination in terrestrial plants. *N. Phytol.* **200**, 950–965 (2013).
74. Richardson, T. B. et al. Carbon dioxide physiological forcing dominates projected Eastern Amazonian drying. *Geophys. Res. Lett.* **45**, 2815–2825 (2018).
75. Song, Y. H., Chung, E.-S., Shahid, S., Kim, Y. & Kim, D. Development of global monthly dataset of CMIP6 climate variables for estimating evapotranspiration. *Sci. Data* **10**, 568 (2023).
76. Longo, M. et al. Degradation and deforestation increase the sensitivity of the Amazon Forest to climate extremes. *Environ. Res. Lett.* **20**, 054024 (2025).
77. Papastefanou, P. et al. Recent extreme drought events in the Amazon rainforest: assessment of different precipitation and evapotranspiration datasets and drought indicators. *Biogeosciences* **19**, 3843–3861 (2022).
78. Miralles, D. G. et al. The WACMOS-ET project – Part 2: Evaluation of global terrestrial evaporation data sets. *Hydrol. Earth Syst. Sci.* **20**, 823–842 (2016).
79. Dutra, D. J. et al. Dry-Season water deficits in the Southwestern Amazon under high emissions. *Int. J. Climatol.* **46**, 70331 (2026).
80. RAISG, A. N. of G. S.-E. I. RAISG 2024. https://www.raisg.org/en/about/ (RAISG, 2024).
81. Sarkar, S. & Maity, R. Global climate shift in 1970s causes a significant worldwide increase in precipitation extremes. *Sci. Rep.* **11**, 11574 (2021).
82. Muñoz-Sabater, J. et al. ERA5-Land: a state-of-the-art global reanalysis dataset for land applications. *Earth Syst. Sci. Data* **13**, 4349–4383 (2021).
83. Duursma, R. A. Plantecophys - An R Package for Analysing and Modelling Leaf Gas Exchange Data. *PLoS One* **10**, e0143346 (2015).
84. R Core Team. *R: A Language and Environment for Statistical Computing*. https://cran.r-project.org/faqs.html (CRAN, 2025).
85. Funk, C. et al. The climate hazards infrared precipitation with stations—a new environmental record for monitoring extremes. *Sci. Data* **2**, 150066 (2015).
86. Polasky, A., Sapkota, V., Forest, C. E. & Fuentes, J. D. Discrepancies in precipitation trends between observational and reanalysis datasets in the Amazon Basin. *Sci. Rep.* **15**, 7268 (2025).
87. dos Santos Silva, F. D. et al. Intercomparison of different sources of precipitation data in the Brazilian Legal Amazon. *Climate* **11**, 241 (2023).
88. Anderson, L. O. et al. Vulnerability of Amazonian forests to repeated droughts. *Philos. Trans. R. Soc. B: Biol. Sci.* **373**, 1–12 (2018).
89. Mu, Y., Biggs, T. & Shen, S. S. P. Satellite-based precipitation estimates using a dense rain gauge network over the Southwestern Brazilian Amazon: implication for identifying trends in dry season rainfall. *Atmos. Res.* **261**, 105741 (2021).
90. Silva-Junior, C. H. L. & Campanharo, W. A. Maximum Cumulative Water Deficit - MCWD: a R language script (v1.1.0) (v1.1.0). Zenodo. https://doi.org/10.5281/zenodo.5034650 (2021).
91. Fasiolo, M., Wood, S. N., Zaffran, M., Nedellec, R. & Goude, Y. QGAM: Bayesian nonparametric quantile regression modelling in R. *J. Stat. Softw*. **100**, 1–31 (2021).

Acknowledgements

We thank the UNSDSN's Science Panel for the Amazon that supported cross fertilisation of ideas between researchers.

Author contributions

J.B. and M.B. conceived the paper. N.S.C. and C.A.N. analysed the data, with additional input from C.H.L.S.J. J.B., N.S.C. and C.A.N. led the writing of the manuscript. A.P.D.A., A.A., L.O.A., L.E.O.C.A., F.B., M.B., E.B., K.B., P.M.B., T.B.A.C., T.F.D., F.E., T.R.F., I.J.M.F., J.N.F., B.M.F., D.G., T.A.G., E.G., M.H., V.K., D.M., C.L., A.C.L., B.L., M.N.M., Y.M., B.S.M., B.H.M.J., P.M., L.M.M., O.M., L.S.M., E.T.A.M., D.C.M., J.N., R.S.O., O.L.P., L.R., J.S., C.V.J.S., C.H.L.S.J., P.S.S., J.M.S., D.V.S., S.S., P.A.T., C.T., I.C.G.V. and H.C.W. contributed to the development of the analysis, the interpretation of results and the writing of the manuscript.

Funding

We thank WWF-UK for funding the core analysis, with key additional support from UKRI's Amazon-SOS (NE/X019039/1) and Rainfauna (NE/X015262/1) projects. JB, EB, JNF, ACL and LMS were also supported by the BNP Paribas Foundation's Climate and Biodiversity initiative, DEFRA's Global Centre for Biodiversity and Climate, and CNPq's Centro Avançado em Pesquisas Socioecológicas para a Recuperação Ambiental da Amazônia (CAPOEIRA - 352886/2025-0) and PELD (445994/2024-0). LMM thanks UKRI projects NE/X001172/1 and NE/W004895/1. TF was supported by UKRI project NE/W001691/1. FE was supported by Serrapilheira Institute (Grant no. R-2401–357 46863) and FAPESPA (TO no. 158/2024). CHLSJ was supported by DEFRA's Global Centre on Biodiversity for Climate (RG2-009854) and the CNPq (Processes 304664/2024-3, 400634/2024-4, 443849/2024-2 and 401741/2023-0). CL and TBAC were supported by UKRI Future Leaders Fellowship (MR/W011085/1). LMS was supported by the Ramboll foundation. TFD was supported by CNPq grant 312589/2022-0 and FAPESP grants 024/08543-8 and 2023/09046-5. BSM and BHMJr were supported by CNPq-PELD 445984/2024-4. ICGV was supported by INCT Nexus (CNPq 406516/2022-7 and FAPESPA -Proc. E-2024/2215630). DML was supported by FAPESP (grant 2023/09046-5) and CNPq (grant 305807/2024-2). PM was also supported by a Royal Society Wolfson Fellowship, RSWF 211008. LOA acknowledges funding from FAPESP project Voices of Recovery (# 2021/07660-2), UKRI's Amazon-SOS (grant no. NE/X019039/1) and CNPq projects CAPOEIRA (#443849/2024-2) and Productivity scholarship (#307364/2025-9).

Competing interests

The authors declare no competing financial interests.

Additional information

Supplementary information The online version contains supplementary material available at https://doi.org/10.1038/s43247-026-03975-1.

Correspondence and requests for materials should be addressed to Jos Barlow, Nathália S. Carvalho or Cássio Alencar Nunes.

Peer review information *Communications Earth & Environment* thanks Wanderson Luiz-Silva and the other, anonymous, reviewers for their contribution to the peer review of this work. Primary Handling Editors: Alireza Bahadori. A peer review file is available.

Reprints and permissions information is available at http://www.nature.com/reprints

Publisher's note Springer Nature remains neutral with regard to jurisdictional claims in published maps and institutional affiliations.

Open Access This article is licensed under a Creative Commons Attribution 4.0 International License, which permits use, sharing, adaptation, distribution and reproduction in any medium or format, as long as you give appropriate credit to the original author(s) and the source, provide a link to the Creative Commons licence, and indicate if changes were made. The images or other third party material in this article are included in the article's Creative Commons licence, unless indicated otherwise in a credit line to the material. If material is not included in the article's Creative Commons licence and your intended use is not permitted by statutory regulation or exceeds the permitted use, you will need to obtain permission directly from the copyright holder. To view a copy of this licence, visit http://creativecommons.org/licenses/by/4.0/.

© The Author(s) 2026

[1]Lancaster Environment Centre, Lancaster University, Lancaster, UK. [2]National Institute for Space Research – INPE, São José dos Campos, Brazil. [3]Amazon Environmental Research Institute (IPAM), Brasília, Brazil. [4]Universidade Federal do Amazonas, Manaus, Brazil. [5]WWF-UK, Surrey, UK. [6]Environmental Change Institute, School of Geography and the Environment, University of Oxford, Oxford, UK. [7]Space Intelligence, Edinburgh, UK. [8]Yale School of the Environment, Yale University, New Haven, CT, USA. [9]School of Environmental Sciences, University of East Anglia, Norwich, UK. [10]Departamento de Biologia - FFCLRP-USP, Ribeirão Preto, Brazil. [11]Embrapa Amazônia Oriental, Belém, Brazil. [12]Faculty of Environment, Science and Economy, University of Exeter, Exeter, UK. [13]EqualSea Lab-CRETUS, University of Santiago de Compostela, A Coruña, Spain. [14]University of Leeds, Leeds, UK. [15]Stockholm Environment Institute, Stockholm, Sweden. [16]Federal University of Santa Catarina, Florianópolis, Brazil. [17]UN Environment Programme World Conservation Monitoring Centre (UNEP-WCMC), Cambridge, UK. [18]Universidade Estadual de Campinas – UNICAMP, Campinas, Brazil. [19]School of Biological and Chemical Sciences, Manchester Metropolitan University, Manchester, UK. [20]Columbia University, New York, NY, USA. [21]State University of Mato Grosso UNEMAT, Nova Xavantina, Brazil. [22]University of Edinburgh, Edinburgh, UK. [23]NASA Goddard Space Flight Center, Greenbelt, MD, USA. [24]Wageningen University & Research, Wageningen, Netherlands. [25]Instituto Nacional de Pesquisas da Amazônia (INPA), Manaus, Brazil. [26]Universidade Federal de Mato Grosso (UFMT), Cuiabá, Brazil. [27]Universidade do Estado do Amapá, Macapá, Brazil. [28]Museu Paraense Emilio Goeldi, Belém, Brazil. [29]WWF-Brazil, Brasília, Brazil. [30]Universidade Federal do Maranhão (UFMA), Sao Luis, Brazil. [31]UK Centre for Ecology & Hydrology, Wallingford, United Kingdom. [32]LEAF, Botany Department, Museu Paraense Emílio Goeldi, Belém, Brazil. [33]TRopical Ecosystems and Environmental Sciences lab (TREES), Earth Observation and Geoinformatics Division, National Institute for Space Research (INPE), São José dos Campos, Brazil. [34]These authors contributed equally: Jos Barlow, Nathália S. Carvalho, Cássio Alencar Nunes. ✉e-mail: jos.barlow@lancaster.ac.uk; nathalia.bioufla@gmail.com; cassioalencarnunes@gmail.com